

Antiferro- and Ferromagnetic Interactions in Mn(II), Co(II), and Ni(II) Compounds with Mixed Azide–Carboxylate Bridges

Yu Ma,[†] Jian-Yong Zhang,[†] Ai-Ling Cheng,[†] Qian Sun,[†] En-Qing Gao,^{*,†} and Cai-Ming Liu[‡]

[†]Shanghai Key Laboratory of Green Chemistry and Chemical Processes, Department of Chemistry, East China Normal University, Shanghai 200062, China, and [‡]Institute of Chemistry, Chinese Academy of Sciences, Beijing 100190, China

Received March 10, 2009

A series of transition metal coordination polymers with azide and flexible zwitterionic dicarboxylate ligands was synthesized and structurally and magnetically characterized. These compounds are formulated as $[M_2(L^1)(N_3)_4]$ ($L^1 = 4,4'$ -trimethylenedipyridinio- N,N' -diacetate and $M = Mn$, **1**; Co , **2**; and Ni , **3**) and $[ML^2(N_3)_6(H_2O)_2]$ ($L^2 = 4,4'$ -dipyridinio- N,N' -diacetate and $M = Mn$, **4**; Co , **5**). The isomorphous compounds **1–3** consist of two-dimensional coordination layers in which the anionic uniform chains with mixed triple bridges (two end-on (EO) azides and a syn–syn carboxylate) are cross-linked by the flexible cationic 4,4'-trimethylenedipyridinium spacers, while the isomorphous compounds **4** and **5** consist of alternating chains with triple (two EO azides plus a carboxylate) and double (two end-to-end azides) bridges, the 4,4'-dipyridinium spacers serving as side bridges along the chain. Magnetic studies demonstrated that the triple bridge transmits antiferromagnetic coupling in the Mn(II) compounds (**1** and **4**) but ferromagnetic coupling in the Co(II) and Ni(II) species (**2**, **3**, and **5**). The differences have been discussed in terms of the collaboration or competition between the carboxylate and azide pathways. Compound **4** exhibits alternating antiferromagnetic interactions, while alternating ferromagnetic–ferromagnetic–antiferromagnetic interactions with spin canting are suggested for **5**.

Introduction

The field of molecular magnetism has attracted much attention and seen great progress in recent years.¹ The systems studied so far consist of extended coordination networks or discrete polynuclear aggregates, in which paramagnetic metal ions are held together by short bridging ligands allowing for sufficiently strong magnetic exchange.^{1–3} In this context, the azide ion, which can adopt versatile

bridging modes (μ -1,1, μ -1,3, μ -1,1,3, etc.) and can efficiently mediate ferromagnetic (FM) or antiferromagnetic (AFM) coupling, has been extensively used in the design of molecular magnets, including many long-range ordering materials and a few single-molecule/-chain magnets (SMMs and SCMs).^{3,4} Much work has been devoted to the control and design of metal–azide systems by incorporating different organic ligands, and the most frequently used auxiliary ligands are neutral molecules bearing one or more heterocyclic N-donor atoms such as pyridyl derivatives.^{3–7} For instance, we have

*To whom correspondence should be addressed. E-mail: eqgao@chem.ecnu.edu.cn.

(1) (a) Kahn, O. *Molecular Magnetism*; VCH: New York, 1993. (b) Miller, J. S. *Adv. Mater.* 2002, 14, 1105. (c) *Magnetism: Molecules to Materials*; Miller, J. S., Drilon, M., Eds.; Wiley-VCH: Weinheim, 2002–2005; Vol. I–V. (d) Gatteschi, D.; Sessoli, R. *Angew. Chem., Int. Ed.* 2003, 42, 268.

(2) (a) Ohba, M.; Okawa, H. *Coord. Chem. Rev.* 2000, 198, 313. (b) Coronado, E.; Day, P. *Chem. Rev.* 2004, 104, 5419. (c) Talham, D. R. *Chem. Rev.* 2004, 104, 5479. (d) Batten, S. R.; Murray, K. S. *Coord. Chem. Rev.* 2003, 246, 103. (e) Lescouezec, R.; Toma, L. M.; Vaissermann, J.; Verdaguer, M.; Delgado, F. S.; Ruiz-Pérez, C.; Lloret, F.; Julve, M. *Coord. Chem. Rev.* 2005, 249, 2691.

(3) (a) Ribas, J.; Escuer, A.; Monfort, M.; Vicente, R.; Cortés, R.; Lezama, L.; Rojo, T. *Coord. Chem. Rev.* 1999, 193, 1027. (b) Wang, X.-Y.; Wang, Z.-M.; Gao, S. *Chem. Commun.* 2008, 281. (c) Escuer, A.; Aromí, G. *Eur. J. Inorg. Chem.* 2006, 4721.

(4) (a) Stamatatos, T. C.; Abboud, K. A.; Wernsdorfer, W.; Christou, G. *Angew. Chem., Int. Ed.* 2007, 46, 844. (b) Zhang, Y.-Z.; Wernsdorfer, W.; Pan, F.; Wang, Z.-M.; Gao, S. *Chem. Commun.* 2006, 3302. (c) Yang, C. I.; Wernsdorfer, W.; Lee, G. H.; Tsai, H. L. *J. Am. Chem. Soc.* 2007, 129, 456. (d) Liu, T.-F.; Fu, D.; Gao, S.; Zhang, Y.-Z.; Sun, H.-L.; Su, G.; Liu, Y.-J. *J. Am. Chem. Soc.* 2003, 125, 13976.

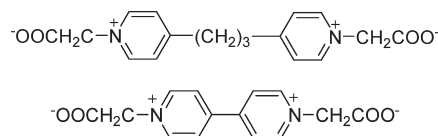
(5) (a) Liu, C.-M.; Gao, S.; Zhang, D.-Q.; Huang, Y.-H.; Xiong, R.-G.; Liu, Z.-L.; Jiang, F.-C.; Zhu, D.-B. *Angew. Chem., Int. Ed.* 2004, 43, 990. (b) Escuer, A.; Mautner, F. A.; Goher, M. A. S.; Abu-Youssef, M. A. M.; Vicente, R. *Chem. Commun.* 2005, 605. (c) Bitschnau, B.; Egger, A.; Escuer, A.; Mautner, F. A.; Sodin, B.; Vicente, R. *Inorg. Chem.* 2006, 45, 868.

(6) (a) Martin, S.; Barandika, M. G.; Lezama, L.; Pizarro, J. L.; Serna, Z. E.; de Larramendi, J. I. R.; Arriortua, M. I.; Rojo, T.; Cortés, R. *Inorg. Chem.* 2001, 40, 4109. (b) Fu, A. H.; Huang, X. Y.; Li, J.; Yuen, T.; Lin, C. L. *Chem.—Eur. J.* 2002, 8, 2239. (c) Wang, X.-Y.; Wang, Z.-M.; Gao, S. *Inorg. Chem.* 2008, 47, 5720. (d) Abu-Youssef, M. A. M.; Langer, V.; Luneau, D.; Shams, E.; Goher, M. A. S.; Ohrström, L. *Eur. J. Inorg. Chem.* 2008, 112.

(7) (a) Gao, E.-Q.; Bai, S.-Q.; Yue, Y.-F.; Wang, Z.-M.; Yan, C.-H. *Inorg. Chem.* 2003, 42, 3642. (b) Gao, E.-Q.; Yue, Y.-F.; Bai, S.-Q.; He, Z.; Yan, C.-H. *J. Am. Chem. Soc.* 2004, 126, 1419. (c) Gao, E.-Q.; Yue, Y.-F.; Bai, S.-Q.; He, Z.; Zhang, S.-W.; Yan, C. H. *Chem. Mater.* 2004, 16, 1590. (d) Gao, E.-Q.; Wang, Z.-M.; Yan, C.-H. *Chem. Commun.* 2003, 1748. (e) Gao, E.-Q.; Cheng, A.-L.; Xu, Y.-X.; He, M.-Y.; Yan, C.-H. *Inorg. Chem.* 2005, 44, 8822. (f) Liu, P.-P.; Cheng, A.-L.; Liu, N.; Sun, W.-W.; Gao, E.-Q. *Chem. Mater.* 2007, 19, 2724. (g) Gao, E.-Q.; Liu, P.-P.; Wang, Y.-Q.; Yue, Q.; Wang, Q.-L. *Chem.—Eur. J.* 2009, 15, 1217.

used dipyriddy and ditetrazole ligands of different lengths and geometries to modulate the bulk magnetic properties of multilayer metal–azide systems.⁷ Considering that the carboxylate group can also efficiently transmit magnetic exchange, combining azide and carboxylate in one system is an interesting approach for constructing new materials and modulating magnetic behaviors. It has been observed that the simultaneous azide and carboxylate bridges in some systems can transmit FM interactions between neighboring metal ions.^{8,9} The observations are particularly interesting for the design of molecular ferromagnets and SCMs. Nevertheless, compared with the large number of azide- or carboxylate-bridged systems, successful examples with simultaneous azide and carboxylate bridges are rather limited, including a few species with simple carboxylates (formate or acetate)^{8,10} and some networks based on a few pyridylcarboxylate derivatives.^{9,11} We are interested in using di- and polycarboxylate ligands and azide to construct high-dimensional networks containing lower-dimensional motifs with short bridges, so that we can study the modulating effects of organic ligands on magnetic behaviors. However, the combination of azide and dicarboxylate ligands seldom succeeded in giving the expected high-dimensional materials with simultaneous azide and carboxylate bridges between neighboring metal ions,¹² perhaps because of the mismatch between azide and dianionic dicarboxylates in the competition to bind metal ions and to compensate the charge of the metal ions. To get the balance, we propose the employment of neutral dicarboxylates as ligands, that is, the inner-salt-type (or zwitterionic) ligands combining two positive pyridinium groups and two negative carboxylate groups, as exemplified by **L**¹ and **L**² in Chart 1. Such ligands are much less explored in coordination chemistry than the common dicarboxylates with neutral spacers and have not been used in the field of molecular magnetic materials. Recently, we have shown that a similar ligand, 1,3-bis(4-carboxylatopyridinium) propane, leads to a novel 3D net based on tetranuclear clusters with simultaneous azide and carboxylate bridges.¹³ Here, we report the synthesis, structures, and magnetic properties of a series of coordination polymers of **L**¹ and **L**² with azide and different transition metal ions. The formulas are [M₂(**L**¹)(N₃)₄] (M = Mn, **1**; Co, **2**; and Ni, **3**) and [ML²(N₃)₆(H₂O)₂] (**L**² = 4,4'-dipyridinio-4,4'-diacetate and M = Mn, **4**, and Co, **5**). Compounds **1**–**3** are isomorphous and consist of 2D

Chart 1. 4,4'-Trimethylenedipyridinio-N,N'-diacetate (**L**¹, top) and 4,4'-Dipyridinio-N,N'-diacetate (**L**², bottom)



coordination networks in which uniform chains with triple bridges (two azides plus a carboxylate) are cross-linked by the flexible 4,4'-trimethylenedipyridinium spacers, while **4** and **5** contain alternating chains with triple (two azides plus a carboxylate) and double (two azides) bridges. Magnetic studies reveal that the triple bridge transmits AFM coupling in the Mn(II) compounds but FM coupling in the Co(II) and Ni(II) species. The difference is discussed, and a spin-canted chain structure is proposed for **5**.

Experimental Section

Physical Measurements. Elemental analyses were determined on an Elementar Vario ELIII analyzer. The FT-IR spectra were recorded in the range 500–4000 cm⁻¹ using KBr pellets on a Nicolet NEXUS 670 spectrophotometer. Temperature-dependent magnetic measurements were carried out on a Quantum Design SQUID MPMS-5 magnetometer with an applied field of 1 or 2 kOe, and diamagnetic corrections were made with Pascal's constants. The phase purity of the samples has been confirmed by powder X-ray diffraction (see the Supporting Information, Figures S1 and S2), which was measured on a Bruker D8 Advance diffractometer equipped with Cu K α at a scan speed of 1° min⁻¹.

Synthesis. The reagents were obtained from commercial sources and used without further purification. The coligands 4,4'-trimethylenedipyridinio-N,N'-diacetate (**L**¹) and 4,4'-dipyridinio-N,N'-diacetate (**L**²) were prepared according to the literature.¹⁴

Caution! Although not encountered in our experiments, azido compounds of metal ions are potentially explosive. The materials should be handled in small amounts and with care.

[Mn₂(L**¹)(N₃)₄] (**1**).** A mixture of MnCl₂·4H₂O (0.1 mmol, 0.020 g), **L**¹ (0.1 mmol, 0.030 g), and NaN₃ (0.2 mmol, 0.013 g) in water/ethanol (4/6 mL) was stirred for 10 min at room temperature. Slow evaporation of the solution at room temperature yielded yellow crystals of **1** within one week. Yield: 45% based on Mn. Anal. found: C, 34.52; H, 3.29; N, 33.13%. Calcd for Mn₂C₁₇H₁₈N₁₄O₄: C, 34.47; H, 3.06; N, 33.11%. Main IR (KBr, cm⁻¹): 2080(s), 2047(m), 1605(m), 1396(m), 1330(w).

[Co₂(L**¹)(N₃)₄] (**2**).** An ethanol solution of CoCl₂·6H₂O (0.1 mmol, 0.024 g) was layered on a mixture of **L**¹ (0.1 mmol, 0.030 g) and NaN₃ (0.2 mmol, 0.013 g) in 5 mL of aqueous solution at room temperature. After 30 days, red crystals of **2** were obtained. Yield: 45% based on Co. Anal. found: C, 33.66; H, 3.50; N, 32.37%. Calcd for Co₂C₁₇H₁₈N₁₄O₄: C, 34.01; H, 3.02; N, 32.67%. Main IR (KBr, cm⁻¹): 2080(s), 2039(m), 1606(m), 1398(m), 1338(w).

[Ni₂(L**¹)(N₃)₄] (**3**).** A mixture of NiCl₂·6H₂O (0.1 mmol, 0.024 g), **L**¹ (0.1 mmol, 0.030 g), and NaN₃ (0.2 mmol, 0.013 g) in water (2 mL) was stirred for 10 min at room temperature, then sealed in a tube and heated at 70 °C for 3 days. After cooling to room temperature slowly, green microcrystals of **3** were obtained. Our efforts to grow single crystals suitable for X-ray crystallographic measurement did not succeed. Yield: 55% based on Ni. Anal. found: C, 33.74; H, 3.40; N, 33.15%. Calcd

(8) (a) Liu, T.; Zhang, Y.-J.; Wang, Z.-M.; Gao, S. *Inorg. Chem.* **2006**, *45*, 2782. (b) Thompson, L. K.; Tandon, S. S.; Lloret, F.; Cano, J.; Julve, M. *Inorg. Chem.* **1997**, *36*, 3301. (c) Wang, X.-T.; Wang, X.-H.; Wang, Z.-M.; Gao, S. *Inorg. Chem.* **2009**, *48*, 1301.

(9) (a) Chen, H.-J.; Mao, Z.-W.; Gao, S.; Chen, X.-M. *Chem. Commun.* **2001**, 2320. (b) He, Z.; Wang, Z.-M.; Gao, S.; Yan, C.-H. *Inorg. Chem.* **2006**, *45*, 6694. (c) Liu, F.-C.; Zeng, Y.-F.; Li, J.-R.; Bu, X.-H.; Zhang, H.-J.; Ribas, J. *Inorg. Chem.* **2005**, *44*, 7298.

(10) (a) Milios, C. J.; Prescimone, A.; Sanchez-Benitez, J.; Parsons, S.; Murrie, M.; Brechin, E. K. *Inorg. Chem.* **2006**, *45*, 7053. (b) Demeshko, S.; Leibeling, G.; Maringele, W.; Meyer, F.; Mennerich, C.; Klauss, H.-H.; Pritzkow, H. *Inorg. Chem.* **2005**, *44*, 519.

(11) (a) Liu, F.-C.; Zeng, Y.-F.; Jiao, J.; Bu, X.-H.; Ribas, J.; Batten, S. R. *Inorg. Chem.* **2006**, *45*, 2776. (b) Zeng, Y.-F.; Zhao, J.-P.; Hu, B.-W.; Hu, X.; Liu, F.-C.; Ribas, J.; Arino, J. R.; Bu, X.-H. *Chem.—Eur. J.* **2007**, *13*, 9924.

(12) (a) Escuer, A.; Vicente, R.; Mautner, F. A.; Goher, M. A. S. *Inorg. Chem.* **1997**, *36*, 1233. (b) Li, L. C.; Liao, D. Z.; Jiang, Z. H.; Yan, S. P. *Polyhedron* **2001**, *20*, 681. (c) Han, Y.-F.; Wang, T.-W.; Song, Y.; Shen, Z.; You, X.-Z. *Inorg. Chem. Commun.* **2008**, *11*, 207. (d) Hong, C. S.; You, Y. S. *Polyhedron* **2004**, *23*, 1379.

(13) Wang, Y.-Q.; Zhang, J.-Y.; Jia, Q.-X.; Gao, E.-Q.; Liu, C.-M. *Inorg. Chem.* **2009**, *48*, 789.

(14) (a) Mao, J.-G.; Zhang, H.-J.; Ni, J.-Z.; Wang, S.-B.; Mak, T. C. W. *Polyhedron* **1999**, *18*, 1519. (b) Fajardo, A. M.; Lewis, N. S. *J. Phys. Chem. B* **1997**, *101*, 11136.

Table 1. Crystal Data and Structure Refinement for Compounds **1**, **2**, **4**, and **5**

	1	2	4	5
empirical formula	Mn ₂ C ₁₇ H ₁₈ N ₁₄ O ₄	Co ₂ C ₁₇ H ₁₈ N ₁₄ O ₄	Mn ₃ C ₁₄ H ₁₆ N ₂₀ O ₆	Co ₃ C ₁₄ H ₁₆ N ₂₀ O ₆
fw	592.33	600.31	725.29	737.26
cryst syst	monoclinic	monoclinic	monoclinic	monoclinic
space group	C2/c	C2/c	C2/c	C2/c
<i>a</i> (Å)	24.5238(9)	24.771(5)	16.1372(16)	15.9219(2)
<i>b</i> (Å)	6.4965(2)	6.2498(12)	13.4945(14)	13.3137(2)
<i>c</i> (Å)	15.3842(5)	15.335(3)	11.8557(12)	11.7049(2)
β (deg)	108.4100(10)	107.53(3)	96.9610(10)	96.6570(10)
<i>V</i> (Å ³)	2325.55(13)	2263.9(8)	2562.7(5)	2464.47(6)
<i>Z</i>	4	4	4	4
<i>D</i> (g m ⁻³)	1.692	1.761	1.880	1.987
μ (mm ⁻¹)	1.144	1.525	1.532	2.076
<i>F</i> (000)	1216	1200	1452	1476
reflns collected	5145	14843	7079	20988
unique reflns	2417	2681	2518	2441
GOF on <i>F</i> ²	0.828	1.064	1.029	1.042
<i>R</i> _{int}	0.0303	0.0747	0.0192	0.0259
<i>R</i> ₁ [<i>I</i> > 2 σ (<i>I</i>)]	0.0266	0.0526	0.0245	0.0198
<i>wR</i> ₂ (all data)	0.0729	0.1408	0.0647	0.0565

for Ni₂C₁₇H₁₈N₁₄O₄: C, 34.04; H, 3.02; N, 32.69%. Main IR (KBr, cm⁻¹): 2080(s), 2040(m), 1605(m), 1397(m), 1337(w).

[MnL²(N₃)₆(H₂O)₂] (**4**). A procedure similar to that for **1** was followed to prepare compound **4**. Within a week, red crystals of **4** were obtained. Yield: 50% based on Mn. Anal. found C, 23.65; H, 2.68; N, 38.83%. Calcd for Mn₃C₁₄H₁₆N₂₀O₆: C, 23.19; H, 2.22; N, 38.63%. Main IR (KBr, cm⁻¹): 2099(s), 2064(s), 2028(m), 1615(s), 1392(m), 1334(w).

[CoL²(N₃)₆(H₂O)₂] (**5**). A procedure similar to that for **2** was followed to prepare compound **5**. Yield: 50% based on Co. Anal. found C, 23.26; H, 2.52; N, 38.04%. Calcd for Co₃C₁₄H₁₆N₂₀O₆: C, 22.81; H, 2.19; N, 38.00%. Main IR (KBr, cm⁻¹): 2098(s), 2062(s), 2028(m), 1615(s), 1392(m), 1338(w).

X-Ray Crystallographic Measurements. Diffraction data for **1**, **2**, **4**, and **5** were collected at 292 K on a Bruker Apex II CCD area detector equipped with graphite-monochromated Mo K α radiation ($\lambda = 0.71073$ Å). Empirical absorption corrections were applied using the SADABS program.¹⁵ The structures were solved by the direct method and refined by the full-matrix least-squares method on *F*², with all non-hydrogen atoms refined with anisotropic thermal parameters.¹⁶ All of the hydrogen atoms attached to carbon atoms were placed in calculated positions and refined using the riding model, and the water hydrogen atoms were located from the difference maps. All calculations were carried out with the SHELXTL crystallographic software. A summary of the crystallographic data, data collection, and refinement parameters for complexes **1**, **2**, **4**, and **5** is provided in Table 1.

Results and Discussion

Synthesis and IR Spectra. The compounds were synthesized by the reaction of MCl₂, NaN₃, and L¹ or L². Compounds **1** and **4** were obtained by slow evaporation of the solution containing the reactants at room temperature. But the same procedure for Co(II) and Ni(II) yielded amorphous filmlike products on the surface of the solution. Pure crystals of compounds **2** and **5** were obtained by layering a solution of CoCl₂ over a mixture solution of L¹ or L² and NaN₃, and microcrystalline samples of **3** were obtained by heating and cooling the aqueous

solution containing all of the reactants in a sealed tube. Although we failed to obtain single crystals of **3** suitable for X-ray crystallographic analysis, the powder X-ray diffraction pattern of the microcrystalline sample of **3** is very similar to those calculated from the crystal data of **1** and **2** (see the Supporting Information, Figure S1), suggesting that **3** is isomorphous with **1** and **2**.

The IR spectra of these complexes display the characteristic bands of the azide and carboxylate groups. The sharp bands in the region of 2100–2020 cm⁻¹ are attributable to the $\nu_{\text{as}}(\text{N}_3)$ vibration, and the $\nu_{\text{s}}(\text{N}_3)$ vibration may be responsible for the weak absorption at about 1330 cm⁻¹. The $\nu_{\text{as}}(\text{COO})$ and $\nu_{\text{s}}(\text{COO})$ vibrations appear as strong bands at about 1610 and 1400 cm⁻¹, respectively.

Crystal Structures. **Compounds 1 and 2.** Compounds **1** and **2** are isomorphous and exhibit 2D coordination networks in which 1D [M(N₃)₂(COO)]_{*n*} chains are interlinked by the zwitterionic L¹ ligands. The relevant parameters are summarized in Table S1 (see Supporting Information). The unique metal ion assumes a trans-octahedral coordination geometry defined by four azide nitrogen atoms (N2, N5, N2A, and N5A) and two carboxylate oxygen atoms (O1 and O2A) (Figure 1). The M–N distances range from 2.203(1) to 2.281(1) Å for **1** and from 2.130(4) to 2.161(4) Å for **2**, while the M–O distances are slightly shorter [2.199(1) and 2.171(1) Å for **1**; 2.136(3) and 2.097(3) Å for **2**]. Adjacent metal ions are triply bridged by two end-on (EO) azide and one syn–syn carboxylate group to generate a uniform chain running along the *b* direction (Figure 2). The neighboring [MN₄O₂] octahedra share the edge defined by two bridging nitrogen atoms and are inclined with respect to each other, with the dihedral angles between the [MN₄] equatorial planes being 153° for **1** and 155° for **2**. The M···M distances spanned by the triple bridge are 3.26 and 3.13 Å for Mn and Co, respectively, and the M–N–M angles for the azide bridges are similar in **1** and **2**, ranging from 93.25(5)° to 93.79(15)°. While no previous analogue is available for Mn(II), the Co–N–Co angles in **2** are slightly smaller than those observed for a previous Co(II) compound with similar triple bridges (two EO azides and a formate Co–N–Co, about 97.4°).^{8a} It is interesting

(15) Sheldrick, G. M. *Program for Empirical Absorption Correction of Area Detector Data*; University of Göttingen: Göttingen, Germany, 1996.

(16) Sheldrick, G. M. *SHELXTL*, version 5.1.; Bruker Analytical X-ray Instruments Inc.: Madison, WI, 1998.

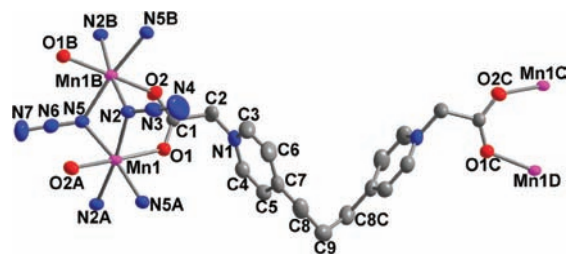


Figure 1. Local coordination environments of the Mn center and the ligands in compound **1**. Hydrogen atoms are omitted for clarity, and the symmetry codes are (A) $0.5 - x, 0.5 + y, 1.5 - z$; (B) $0.5 - x, -0.5 + y, 1.5 - z$; (C) $1 - x, y, 2.5 - z$; (D) $0.5 + x, -0.5 + y, 1 + z$.

to note that the M–N–M angle in mixed azide–carboxylate bridging systems is dependent upon the relative number of the azide and carboxylate bridges. The parameters in the above triple-bridge systems are below the usual range of $99\text{--}107^\circ$ for previous M(II) systems (M = Mn, Ni, or Co) with double EO azide bridges,^{3,7e,17} in which the four-membered $[\text{M}(\text{N})_2\text{M}]$ ring motif is usually planar. This can be well understood as follows: the incorporation of the syn–syn carboxylate bridge causes the neighboring coordination octahedra to incline toward each other. This is accompanied by the folding of the $[\text{M}(\text{N})_2\text{M}]$ ring along the N \cdots N diagonal and, hence, leads to a nonplanar $[\text{M}(\text{N})_2\text{M}]$ ring with decreased M–N–M angles. By contrast, the bridging angle is significantly expanded to about 120° if an azide bridge in the double EO azide system is replaced by a carboxylate bridge, as observed for a few Mn(II), Ni(II), and Co(II) compounds with double azide–carboxylate bridges.^{9a,9b}

All of the $[\text{M}(\text{N}_3)_2(\text{COO})^-]_n$ chains are parallel, and neighboring chains are interlinked by the dicarboxylate L ligands, which adopt the μ_4 -tetradentate coordination mode. Thus, a 2D layer is formed. The ligand, with its central carbon atom (C9) residing on a 2-fold axis, assumes a spiral conformation with the trimethylene spacer in the gauche–gauche conformation. The nearest interchain M \cdots M distances within the layer are $16.120(1)$ Å for **1** and $16.679(1)$ Å for **2**. The layers are packed in parallel with weak interlayer hydrogen bonds, which involve the C–H group from one layer and the carboxylate O atom or azide N atom from the other layer (see the Supporting Information, Figure S3). The nearest interlayer M \cdots M distances are $7.616(1)$ Å for **1** and $7.717(4)$ Å for **2**.

Compounds 4 and 5. Compounds **4** and **5** are isomorphous and contain 1D neutral polymeric chains that are different from those in **1** and **2**. Here, the two structures are described together for the convenience of comparison, and the relevant parameters are summarized in Table S2 (see Supporting Information). As shown in Figure 3, there are two crystallographically independent M(II) atoms. The M2 atom resides on an inversion center and assumes a trans-octahedral coordination geometry similar to that observed in **1** and **2**, with four equatorial nitrogen atoms (N5, N8, N5A, and N8A) from four EO azide ions (average M–N = $2.225(2)$ Å for **4** and $2.136(1)$ Å for **5**) and two axial oxygen atoms (O2 and

O2A) from different carboxylate groups (M–O = $2.185(1)$ Å for **4** and $2.108(1)$ Å for **5**). Differently, M1 assumes a cis-octahedral geometry completed by two nitrogen atoms (N5 and N8) from two EO azide ions, another two nitrogen atoms (N1 and N3) from two end-to-end (EE) azide ions, a carboxylate oxygen atom (O1), and a water molecule (O3). The M1–N(O) bond distances fall in the ranges between 2.14 and 2.26 Å for **4** and between 2.08 and 2.18 Å for **5**. As found in **1** and **2**, the M2 and M1 atoms are triply linked by two EO azide bridges and a syn–syn carboxylate bridge, with similar bridging angles (M1–N–M2 = $93.81\text{--}94.31^\circ$). Through such bridges, each M2 is linked to two M1 atoms to form a linear trinuclear motif. Neighboring M1 atoms from different trinuclear units are doubly linked by two EE azide bridges, and hence an infinite chain is formed along the (10-1) direction, in which the triple (two EO azides plus a carboxylate) and double (two EE azides) bridges alternate in the triple–triple–double sequence. To our knowledge, such a bridging network is unprecedented in the literature. The M1 \cdots M2 distances spanned by the triple bridge are 3.22 Å for **4** and 3.12 Å for **5**, comparable to those in **1** and **2**, while the M1 \cdots M1 distances spanned by the double bridge are much longer (5.19 Å for **4** and 5.11 Å for **5**). In the doubly bridged M(EE-N₃)₂M motif, the two independent EE azide bridges share a common two-fold axis passing through their central atoms and have similar M–N–N angles in the narrow range of $123.3\text{--}124.6^\circ$ but form quite different M–NNN–M torsion angles (85.1 versus 51.2° for **4** and 85.3 versus 51.3° for **5**). We note that the eight-membered M(EE-N₃)₂M motif assumes an uncommon conformation. For most compounds with double EE-azide bridges, the motif takes a chair conformation with the two bridges being (pseudo)parallel (and coplanar). However, the two EE azide bridges in **4** and **5** are noncoplanar with a cross angle of about 47° , defining a twisted conformation for the M(EE-N₃)₂M motif. Such a conformation has only been previously recognized in a few Ni(II) and Mn(II) species.¹⁸

Similar to L¹ in **1** and **2**, the 4,4'-dipyridinium-based ligand (L²) in **4** and **5** also serves as a μ_4 -tetradentate bridge via its two carboxylate groups. It is bisected by a crystallographic two-fold axis passing through the midpoint of the central C–C bond, and the two pyridyl rings are relatively rotated by a dihedral angle of about 40.5° . The two carboxylate groups are arranged at the same side of the 4,4'-bipyridinium moiety so that a U-shaped conformation is generated, and the length between the two carboxylate groups matches well with the distance spanned by two triple bridges and a double one along the metal–azide chain. This allows the ligand to connect four metal ions from the same chain and hence to serve as side bridge between adjacent trinuclear motifs along the chain. Such a bridging mode of L² does not lead to an increase in dimensionality of the coordination structure. This is in contrast to the trimethylenedipyridinium-based

(17) (a) Yu, M.-M.; Ni, Z.-H.; Zhao, C.-C.; Cui, A.-L.; Kou, H.-Z. *Eur. J. Inorg. Chem.* **2007**, 5670. (b) Bai, S.-Q.; Gao, E.-Q.; He, Z.; Fanga, C.-J.; Yan, C.-H. *New J. Chem.* **2005**, 29, 935.

(18) (a) Gao, E.-Q.; Liao, D.-Z.; Jiang, Z.-H.; Yan, S.-P.; Zhang, S.-F. *Acta Chim. Sin.* **2001**, 59, 1294. (b) Chaudhuri, P.; Weyhermüller, T.; Bill, E.; Wieghardt, K. *Inorg. Chim. Acta* **1996**, 252, 195. (c) Vicente, R.; Escuer, A.; Ribas, J.; Solans, X. *Inorg. Chem.* **1992**, 31, 1726. (d) Monfort, M.; Resino, I.; Ribas, J.; Solans, X.; Font-Bardia, M.; Rabu, P.; Drillon, M. *Inorg. Chem.* **2000**, 39, 2572.

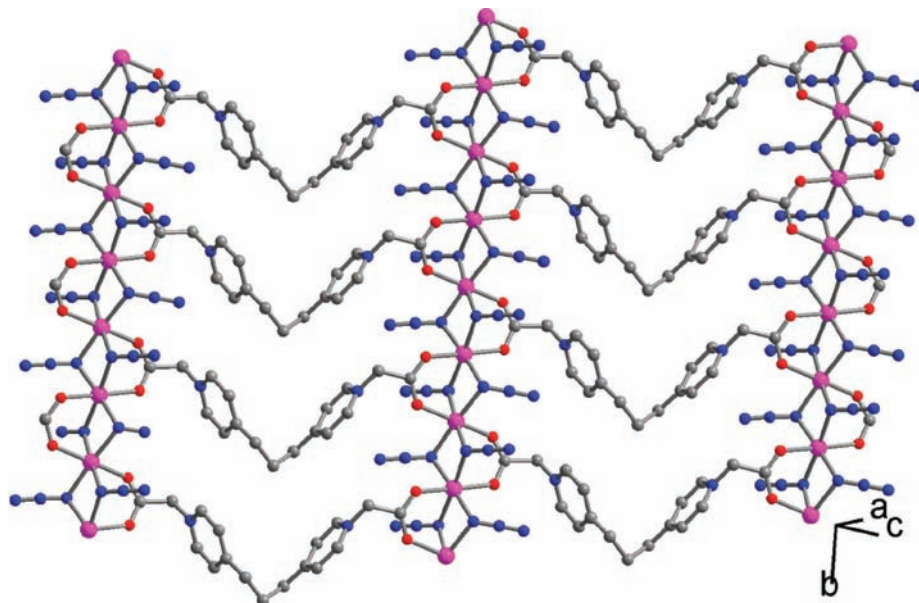


Figure 2. 2D network in **1** formed by the L^1 ligands connecting the uniform chains with mixed triple bridges.

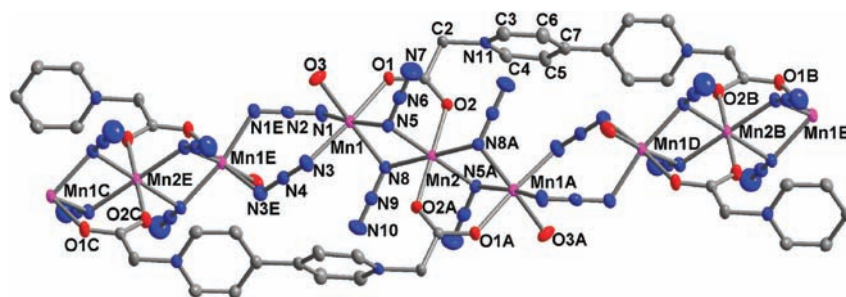


Figure 3. Local coordination environments of the Mn centers and the ligands in compound **4**. Hydrogen atoms are omitted for clarity and symmetry codes are (A) $0.5 - x, 0.5 - y, 2 - z$; (B) $1 - x, y, 1.5 - z$; (C) $-0.5 + x, 0.5 - y, 0.5 + z$; (D) $0.5 + x, 0.5 - y, -0.5 + z$; (E) $-x, y, 2.5 - z$.

ligand (L^1), which adopts a divergent spiral conformation and links the azide-bridged chains into 2D networks. The difference may be related to the presence of the flexible alkyl spacers in L^1 and the match of the length of L^2 with the trinuclear motif in **4** and **5**.

All of the chains in **4** and **5** are aligned in parallel and stacked into 3D architectures through $O3-H \cdots O1$ and $O3-H \cdots N7$ hydrogen bonds, which are formed by the coordinated water molecule ($O3$) from one chain donating its hydrogen atoms to a carboxylate oxygen atom ($O1$) and an EO-azide nitrogen atom ($N7$) from two neighboring chains. Through these hydrogen bonds, each chain is associated with six neighbors (see the Supporting Information, Figure S4). The nearest interchain $M \cdots M$ distances are 5.36 Å for **4** and 5.29 Å for **5**.

Magnetic Properties. Compound 1. The magnetic susceptibility (χ) of compound **1** was measured on a crystal-line sample under 1 kOe in the range of 2–300 K (Figure 4). The χT value per Mn^{II} at 300 K is about $3.76 \text{ emu K mol}^{-1}$, lower than the value expected for a magnetically isolated $Mn(II)$ ion ($4.38 \text{ emu K mol}^{-1}$). As the temperature is lowered, the χT value decreases continuously, while the χ value first increases to a broad maximum at 16 K, then decreases until 3 K, and finally increases slightly again. The data above 100 K follow the Curie–Weiss law with $C = 4.31 \text{ emu K mol}^{-1}$ and $\theta = -42.8 \text{ K}$. The above features all indicate an AFM

coupling between the $Mn(II)$ centers, except the slight increase of χ below 3 K, which could be attributed to the paramagnetic impurity.

According to the structural data, the system can magnetically be treated as an infinite uniform chain in which magnetic coupling is mediated through the triple bridge (two EO azides and a syn–syn carboxylate). The inter-chain magnetic interactions through the long organic ligand and hydrogen bond should be negligible. Consequently, the interaction (J) through the triple bridge can be evaluated by the conventional equation derived by Fisher for a uniform chain of classical spins based on the Hamiltonian $H = -J \sum S_i S_{i+1}$:¹⁹

$$\chi = [Ng^2\beta^2 S(S+1)/(3kT)][(1+u)/(1-u)](1-\rho) + Ng^2\beta^2 S(S+1)\rho/(kT)$$

where u is the well-known Langevin function defined as $u = \coth[JS(S+1)/kT] - kT/[JS(S+1)]$ with $S = 5/2$, and ρ is the molar fraction of the paramagnetic impurity presumed to be mononuclear species. The best simulation leads to $J = -4.7 \text{ cm}^{-1}$ and $\rho = 0.0015$ with g fixed at 2.00 (Figure 4).

(19) Fisher, M. E. *Am. J. Phys.* **1964**, *32*, 343.

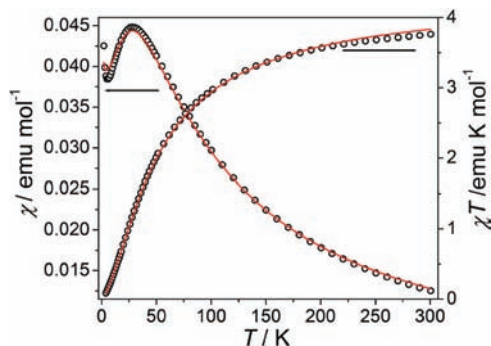


Figure 4. Temperature dependence of χ and χT for **1** under 1 kOe. The red solid lines represent the best fit to the Fisher model (see text).

Compounds 2 and 3. These two compounds display similar magnetic properties (Figures 5 and 6). The room-temperature χT value is $3.44 \text{ cm}^3 \text{ K mol}^{-1}$ for **2**, much larger than the spin-only value ($1.88 \text{ cm}^3 \text{ K mol}^{-1}$) for $S = 3/2$, as expected for Co(II) systems with a significant contribution from the unquenched orbital momentum in the octahedral field (the $^4T_{1g}$ state). For **3**, the room-temperature χT value ($1.37 \text{ cm}^3 \text{ K mol}^{-1}$) is typical of Ni(II) systems with $g > 2$. As the temperature is lowered, the χ values for both compounds increase monotonically, while the χT values increase to sharp maxima at 3 K of $14.65 \text{ emu K mol}^{-1}$ for **2** and of $9.25 \text{ emu K mol}^{-1}$ for **3** and then decrease rapidly upon further cooling. The increase of χT with decreased temperature clearly indicates FM coupling interactions between the metal centers. For **2**, it should be noted that the effects of spin-orbital coupling and the ligand-field distortion, which would lead to a decrease of χT with decreased temperature, are overtaken by the effect of FM interactions. The final decrease of χT for both compounds may be attributed to the saturation effect or the presence of interchain AFM interactions. The data above 120 K for both compounds follow the Curie–Weiss law with $C = 3.16 \text{ emu K mol}^{-1}$ and $\theta = 24.7 \text{ K}$ for **2** and $C = 1.24 \text{ emu K mol}^{-1}$ and $\theta = 30.7 \text{ K}$ for **3**. The positive θ values confirm the FM coupling between metal centers, and the C values fall in the usual ranges expected for Co(II) and Ni(II). The FM coupling is also supported by the isothermal magnetizations measured at 2 K (Figure 6), which rise very rapidly in the low field region. The magnetization of **3** reaches a saturation value of $2.18 \text{ N}\beta$ at 50 kOe, which agrees well with the values ($gS \text{ N}\beta$) expected for Ni(II) with $g = 2.1\text{--}2.3$.²⁰ The magnetization of **2** is $2.64 \text{ N}\beta$ at 50 kOe, which is in the usual range of $2\text{--}3 \text{ N}\beta$ for Co(II).^{20,21} It is noted that the value of **2** tends to increase slowly upon further increasing of the field above 50 kOe. This behavior is typical of Co(II) systems with a larger magnetic anisotropy. Further magnetic measurements revealed no indications of long-range ordering or single-chain slow relaxation behaviors (no hysteresis and no out-of-phase ac susceptibility signals, Figures S5 and S6, Supporting Information).

Because of the low spin values in **2** and **3** and the large magnetic anisotropy of **3**, the Fisher model we used for **1**

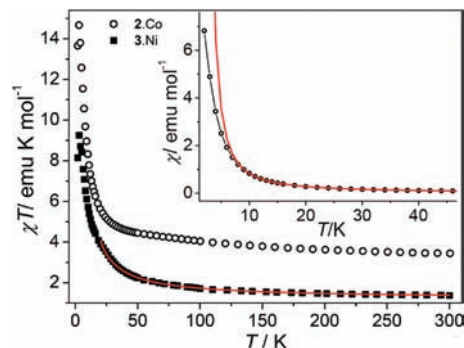


Figure 5. Temperature dependence of χT for **2** and **3** under 1 kOe. Inset: temperature dependence of χ in the low-temperature region for **2**. The red solid lines represent the fit to appropriate models (see text).

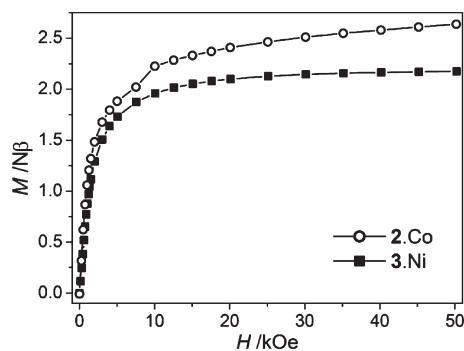


Figure 6. Field-dependent isothermal magnetization curves for compounds **2** and **3** at 2 K (the solid lines are only the guide for the eye).

is not applicable to **2** and **3**. Alternative models are used to evaluate the FM interactions. It is well-known that octahedral cobalt(II) may be handled as an Ising-like ion with effective $S = 1/2$ spin at low temperatures. Thus, the fit of the low-temperature χ data between 9 and 40 K to the Ising chain model was attempted using the following expressions based on the Hamiltonian $H = -J\sum S_i S_{i+1}$:^{8a,22}

$$\chi = (\chi_{\parallel} + 2\chi_{\perp})/3$$

with

$$\chi_{\perp} = (N\beta^2 g_{\perp}^2 / 4kT) \exp(J/2kT)$$

$$\chi_{\parallel} = (N\beta^2 g_{\parallel}^2 / 2J) [\tanh(J/4kT) + (J/2kT) \operatorname{sech}^2(J/4kT)]$$

The data between 9 and 40 K are well simulated by the expressions with $J = 10.7 \text{ cm}^{-1}$, $g_{\parallel} = 11.1(1)$, and $g_{\perp} = 0$ (Figure 5, inset). The J value is comparable with that reported for a previous Co(II) compound with similar triple bridges (two azides and a formate, $J = 13.9 \text{ cm}^{-1}$),^{8a} and the zero value of g_{\perp} confirms the strong Ising-like anisotropy of the system. The relationship that $\chi T (= \chi_{\parallel} T/3) \propto \exp(-J/kT)$ suggests that the $\ln(\chi T)$ value

(20) Carlin, R. L. *Magnetochemistry*; Springer-Verlag: Berlin, 1986.

(21) Yoo, H. S.; Kim, J. I.; Yang, N.; Koh, E. K.; Park, J.-G.; Hong, C. S. *Inorg. Chem.* **2007**, *46*, 9054.

(22) (a) Fisher, M. E. *J. Math. Phys.* **1963**, *4*, 124. (b) Sato, M.; Kon, H.; Akoh, H.; Tasaki, A.; Kabuto, C.; Silverton, J. V. *Chem. Phys.* **1976**, *16*, 405.

in the range 9–40 K increases linearly with $1/T$. This behavior is characteristic for 1D systems with uniaxial anisotropy.²³ The deviation from the Ising model at lower temperatures may be attributed to the possible interchain weak AFM interactions or the finite-size effects related to the defects limiting the correlation length along the chain.

For **3**, the data were analyzed using the empirical polynomial expression proposed by $H = -J\sum S_i S_{i+1}$ for FM Ni(II) chains:²⁴

$$\chi = (2N\beta^2 g^2 / T)(AX^3 + BX^2 + CX + 1) / 3k(DX^2 + EX + 1)$$

where $X = J/kT$, and the coefficients are $A = 0.14709$, $B = -0.788967$, $C = 0.866426$, $D = 0.096573$, and $E = -0.624929$. The best fit of the data above 20 K produced $J = 19.4 \text{ cm}^{-1}$ with $g = 2.21$. The J value suggests a medium FM interaction through the triple bridge. The J parameter is comparable with that for a similar triple bridge in a recently reported Ni(II) compound, which contains alternating triple and single bridges.^{8c}

The magnetic analyses on compounds **1–3** bring us to an interesting issue concerning the nature of magnetic interactions for different metal ions. Structurally, these compounds are isomorphic and contain almost identical chains in which neighboring metal ions are triply linked by two EO azide bridges and a syn–syn carboxylate bridge, with only minor differences in bond parameters. Magnetically, the Mn(II) compound displays AFM coupling through the triple bridge, while FM coupling is observed in the Co(II) and Ni(II) species. Generally, the overall magnetic coupling in systems with coexistent bridges is the concurrent effect of the collaborative or competitive pathways. Experimental and theoretical studies have established that the syn–syn carboxylate bridge is a universal AFM pathway because it induces a good overlap of magnetic orbitals.²⁵ For the EO azide bridge, density function theory (DFT) calculations²⁶ on Cu(II), Ni(II), and Mn(II) systems suggested that the nature of the exchange is dependent upon the M–N–M bridging angle (θ) and the crossover between FM and AFM behaviors occurs at different angles for different metal ions. For Mn(II), the crossover is predicted at $\theta \approx 98^\circ$. While the FM zone ($\theta > 98^\circ$) has been experimentally verified in some Mn(II) compounds containing double EO azide bridges,^{3a,17a} no examples have been reported for the AFM zone ($\theta < 98^\circ$), which was predicted to be energetically unstable for double EO azide bridges.²⁶ Interestingly, in our case (compound **1**), the incorporation of a carboxylate bridge leads to decreased θ values (about 93.5°) for the two azide bridges, and according to the theoretical prediction, AFM exchange might be operative through the azide bridges. Therefore, all of the

pathways in **1** are anticipated to transmit AFM exchange, resulting in the observed AFM coupling. It is noted that AFM coupling has also been reported in three previous Mn(II) compounds that have azide and carboxylate bridges between adjacent metal ions.^{9a,9b} The θ angles for these double-bridge compounds are about 120° , and thus the azide bridge is expected to promote FM exchange. The observed AFM interaction suggests that the AFM pathway through carboxylate overtakes the FM one through azide. This consideration is supported by the fact that the J values (-1.5 to -2.5 cm^{-1}) for the double bridge^{9a,9b} are significantly smaller than that for the triple bridge in **1** (-4.7 cm^{-1}).

A number of Ni(II) compounds containing EO azide bridges have been structurally and magnetically characterized. The double-bridged moieties $[\text{Ni}(\text{N}_3)_2\text{Ni}]$ generally exhibit θ angles in the range of 95 – 105° and J values between $+27$ and $+73 \text{ cm}^{-1}$.^{3a,27} The θ angle can be reduced to 85° in triple-azide-bridged systems²⁸ or expanded to 129° in some mixed bridged systems,^{10b,29,30} and the coupling is always FM. The DFT studies on double-bridged systems suggested that the crossover from FM to AFM behaviors would occur at a low angle of $\theta \approx 75^\circ$, which is believed to be experimentally unattainable.²⁶ Thus, the EO azide has been considered as an almost universal FM pathway.³⁰ In our case, considering the isomorphism of **1–3**, the θ angles in the Ni(II) compound (**3**) should be close to 93° . It is likely that the FM exchange promoted by the two EO azide bridges overtakes the AFM exchange through the carboxylate, resulting in the observed FM behavior in **3**. It is noted that FM coupling has also been reported in previous Ni(II) compounds with double azide–carboxylate bridges.^{9b,9c} These compounds exhibit larger J values (25 – 36 cm^{-1}) than **3**. This seems in disagreement with the expectation that the FM contribution should be reduced when going from the triple bridge to the double bridge. To address this, it might be speculated that the azide-mediated FM coupling associated with the larger θ angles (121 – 125°) in the double-bridged systems is stronger than that corresponding to the smaller θ angles in **3**, or that the carboxylate-mediated AFM coupling associated with the longer M···M distances in the double-bridged systems is weaker than that in **3**.

No theoretical calculations on azide-bridged Co(II) systems are available, perhaps owing to the complexity and difficulty arising from the strong anisotropy. As far as the sign of the magnetic coupling is concerned, the present Co(II) system is similar to the Ni(II) system; that is, the FM exchange promoted by the two EO azide bridges overtakes the AFM exchange through the carboxylate bridge, resulting in the observed FM behavior in **2**. FM interactions through double azide bridges have been reported in a few Co(II) species.^{4d,17b}

(23) Coulon, C.; Miyasaka, H.; Clérac, R. *Struct. Bonding (Berlin)* **2006**, *122*, 163.

(24) Monfort, M.; Resino, I.; Fallah, M. S. E.; Ribas, J.; Solans, X.; Font-Bardia, M.; Stoeckli-Evans, H. *Chem.—Eur. J.* **2001**, *7*, 280.

(25) (a) Cauchy, T.; Ruiz, E.; Alvarez, S. *J. Am. Chem. Soc.* **2006**, *128*, 15722. (b) Rodríguez-Fortea, A.; Alemany, P.; Alvarez, S.; Ruiz, E. *Chem.—Eur. J.* **2001**, *7*, 627. (c) Maji, T. K.; Sain, S.; Mostafa, G.; Lu, T.-H.; Ribas, J.; Monfort, M.; Chaudhuri, N. R. *Inorg. Chem.* **2003**, *42*, 709.

(26) Ruiz, E.; Cano, J.; Alvarez, S.; Alemany, P. *J. Am. Chem. Soc.* **1998**, *120*, 11122.

(27) Sarkar, S.; Mondal, A.; Fallah, M. S. E.; Ribas, J.; Chopra, D.; Stoeckli-Evans, H.; Rajak, K. K. *Polyhedron* **2006**, *25*, 25.

(28) (a) Chaudhuri, P.; Weyhermiller, T.; Bill, E.; Wieghardt, K. *Inorg. Chim. Acta* **1996**, *252*, 195. (b) Beer, P. D.; Drew, M. G. B.; Leeson, P. B.; Lyssenko, K.; Ogden, M. I. *J. Chem. Soc., Chem. Commun.* **1995**, 929.

(29) Meyer, F.; Demeshko, S.; Leibel, G.; Kersting, B.; Kaifer, E.; Pritzkow, H. *Chem.—Eur. J.* **2005**, *11*, 1518.

(30) Mialane, P.; Dolbecq, A.; Rivière, E.; Marrot, J.; Sécheresse, F. *Angew. Chem., Int. Ed* **2004**, *43*, 2274.

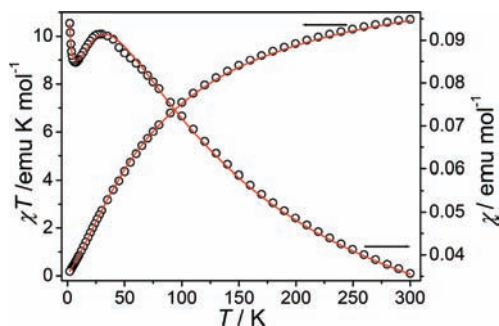


Figure 7. Temperature dependence of χ and χT for **4** under 1 kOe. The red solid lines represent the best fit to the equation for classical-spin chains with alternating $J_1-J_1-J_2$ interactions (see text).

The change of magnetic coupling from FM to AFM for different divalent metal ions in the present isostructural series is similar to that found in the metal dicyanamide series of $M[N(CN)_2]_2$, where the coupling through the $N-C\equiv N$ bridging moiety is FM for $M = Co$ and Ni but AFM for $M = Mn$ and Fe .^{2d,31} On the basis of a Goodenough-type superexchange model,^{31d} Kurmoo related the magnetic change in the dicyanamide series to the different $t_{2g}^x e_g^y$ configurations for the octahedral metal centers.^{31a,31b} It was proposed that the $t_{2g}-e_g$ superexchange between the metal ions is AFM, while the $t_{2g}-t_{2g}$ and e_g-e_g combinations are FM. The relative number and magnitude of these exchange contributions determine the nature of the overall coupling. From $Ni(t_{2g}^6 e_g^2)$, no $t_{2g}-t_{2g}$ and $t_{2g}-e_g$ contributions to $Mn(t_{2g}^3 e_g^3)$, the AFM $t_{2g}-e_g$ contributions increase more rapidly with the removal of electrons from the t_{2g} orbitals and finally dominate over the FM contributions. Our series for the triple azide-carboxylate bridge is consistent with these considerations.

Compound 4. The temperature-dependent magnetic susceptibilities of compound **4** were measured under 1 kOe in the range of 2–300 K (Figure 7). The χT value per formula at 300 K is about $10.71 \text{ emu K mol}^{-1}$, lower than the spin-only value ($13.14 \text{ emu K mol}^{-1}$) expected for three magnetically isolated $Mn(II)$ ions. The general variations of χT and χ with the temperature are similar to those for compound **1**, but the maximum and the minimum of the $\chi(T)$ plot occur at higher temperatures, 29 and 7 K, respectively. The data above 100 K follow the Curie–Weiss law with $C = 14.0 \text{ emu K mol}^{-1}$ and $\theta = -90.7 \text{ K}$, indicating global AFM coupling in the compound. The increase of χ below 7 K could also be attributed to the paramagnetic impurity.

The structural study revealed that the compound contains chains in which triple (two EO azides plus a carboxylate) and double (two EE azides) bridges alternate in the triple–triple–double sequence. The triple bridge motif is structurally very similar to that in **1**, so we can safely assume that AFM coupling is mediated by the triple bridge, as revealed by the magnetic study on **1**. The

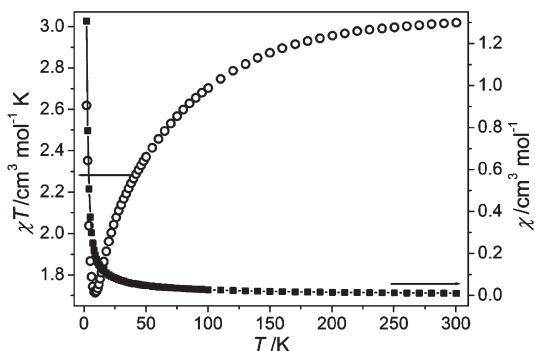


Figure 8. Temperature dependence of χ and χT for **5** under 1 kOe (the solid line is only a guide for the eye).

double EE azide bridge should also mediate AFM coupling according to a number of studies on $Mn(II)$ systems with such bridges.^{7a,32} To evaluate the interactions, we used the theoretical model derived for classical-spin chains with alternating $J_1-J_1-J_2$ interactions, which is described by the spin Hamiltonian $H = -J_2 \sum (S_{3i} S_{3i+1} + S_{3i+1} S_{3i+2}) - J_1 \sum S_{3i-1} S_{3i}$.³³ Taking into account the presence of any paramagnetic impurity, the expression is

$$\chi = [Ng^2\beta^2 S(S+1)/(3kT)](A/B)(1-\rho) + Ng^2\beta^2 S(S+1)\rho/(kT)$$

with

$$A = 3(1-u_1^4 u_2^2) + 4u_1(1-u_1^2 u_2^2) + 2u_2(1+u_1)^2(1-u_1^2) + 2u_1^2(1-u_2^2)$$

and

$$B = (1-u_1^2 u_2^2)^2$$

where $u_i = \coth[J_i S(S+1)/kT] - kT/[J_i S(S+1)]$ ($i = 1, 2$) with $S = 5/2$, and ρ is the molar fraction of the paramagnetic impurity presumed to be mononuclear species. With g fixed at 2.00, the best-fit parameters are $J_1 = -5.6 \text{ cm}^{-1}$, $J_2 = -11.2 \text{ cm}^{-1}$, and $\rho = 0.0023$. The J_1 value is in good agreement with the value obtained for the similar triple bridge in **1**, and the J_2 value falls within the range of -6 to -17 cm^{-1} observed for double EE bridges in previous $Mn(II)$ species.^{7a,32}

Compound 5. The χT values per formula for **5** at 300 K are about $9.06 \text{ emu K mol}^{-1}$, falling in the range expected for three $Co(II)$ ions with a significant contribution from the unquenched orbital momentum. As the temperature is lowered, the χT value decreases smoothly to a minimum at 9 K and then increases sharply, while the χ value shows a monotonic increase (Figure 8). The data above 50 K follow the Curie–Weiss law with $C = 9.66 \text{ emu K mol}^{-1}$ and $\theta = -18.5 \text{ K}$. The temperature-dependent behavior should be owing to the interplay of local magnetic effects

(31) (a) Batten, S. R.; Jensen, P.; Kepert, C. J.; Kurmoo, M.; Moubarak, B.; Murray, K. S.; Price, D. J. *J. Chem. Soc., Dalton Trans.* **1999**, 2987. (b) Kmety, C. R.; Huang, Q.; Lynn, J. W.; Erwin, R. W.; Manson, J. L.; McCall, S.; Crow, J. E.; Stevenson, K. L.; Miller, J. S.; Epstein, A. J. *Phys. Rev.* **2000**, *B 62*, 5576. (c) Nuttall, C. J.; Takenobu, T.; Iwasa, Y.; Kurmoo, M. *Mol. Cryst. Liq. Cryst.* **2000**, *342*, 227. (d) Goodenough, J. B. *Magnetism and the Chemical Bond*; Wiley: New York, **1963**.

(32) Bai, S.-Q.; Gao, E.-Q.; He, Z.; Fang, C.-J.; Yue, Y.-F.; Yan, C.-H. *Eur. J. Inorg. Chem.* **2006**, 2, 407.

(33) (a) Abu-Youssef, M. A. M.; Escuer, A.; Goher, M. A. S.; Mautner, F. A.; Reib, G. J.; Vicente, R. *Angew. Chem., Int. Ed.* **2000**, *39*, 1624. (b) Abu-Youssef, M. A. M.; Drillon, M.; Escuer, A.; Goher, M. A. S.; Mautner, F. A.; Vicente, R. *Inorg. Chem.* **2000**, *39*, 5022.

(including spin–orbital coupling and ligand-field distortion) of Co(II) and magnetic interactions between Co(II) ions. With no suitable model for such a complex system with alternating bridges, we were unable to evaluate the relevant parameters, but some tentative comments can be made on the nature of the magnetic interactions. The triple bridge consisting of two azides and a carboxylate should mediate FM coupling, considering the structural similarity of the bridge to that in **2**, and the interaction through the double EE azide bridge must be AFM. Compared to Mn(II) and Ni(II) species, Co(II) compounds with double EE azide bridges are very rare.³⁴ Recently, a uniform chain with such bridges has been reported to exhibit AFM behaviors.^{34a} In the alternating system of **5**, the overall decrease of χT upon cooling to 9 K simply suggests that the FM coupling is overcompensated by the local magnetic effects and the AFM coupling.

The rapid increase of χT below 9 K needs additional comments. The alternating FM–FM–AFM interactions along the chain should lead to a nonmagnetic ground state ($S = 0$) at very low temperatures, as illustrated in Chart 2b. The χT product of such a system should show a continuous decrease upon cooling to very low temperatures. The low-temperature rise of χT in **5** implies the presence of some ferromagnetic-like correlation in the system. This abnormal behavior is also observed in isothermal magnetization measurements at 2 K (Figure 9). The magnetization (3.77 N β per formula or 1.26 N β per Co) at 50 kOe is much lower than expected (2–3 N β per Co).²⁰ For comparison, the value of **2** is 2.64 N β per Co, and the value tends to rise steadily above 50 kOe. This is consistent with the overall AFM nature in **5**. Nevertheless, the rapid increase of the magnetization in the low-field region is atypical of AFM systems and inconsistent with the alternating FM–FM–AFM interactions in **5**, implying the presence of some ferromagnetic-like correlation.

To explain the phenomena, a spin-canting structure might be proposed. As is well established, spin canting can arise from two mechanisms:^{20,35} (i) single-ion magnetic anisotropy, which energetically favors spin canting if the anisotropy axes on neighboring sites are different, and (ii) the antisymmetric Dzyaloshinsky–Moriya interaction, which tends to align the interacting spins in a perpendicular way and requires g -factor anisotropy. Both mechanisms require that there be no inversion centers between adjacent metal ions. In **5**, the adjacent Co(II) ions (and the triply bridged FM trinuclear units) linked by the double EE azide bridge are related by a C_2 axis, and the corresponding metal chromophores are tilted toward each other with the equatorial planes forming a dihedral angle of 74.2°. This structural feature, together with the strong magnetic anisotropy of pseudo-octahedral Co(II), fulfills the requirements for spin canting. Therefore, the AFM coupled spins (or the spins from neighboring trimeric units) are not perfectly antiparallel. An illustrative pattern of the spin canting along the chain is given in Chart 2c. At low temperatures, the thermal energy is not

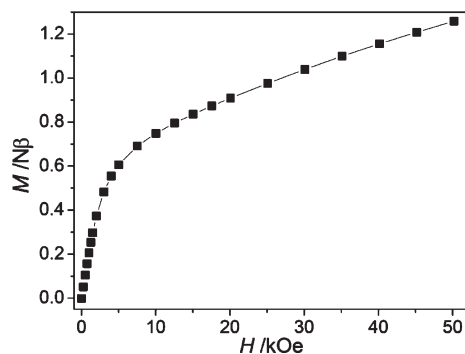
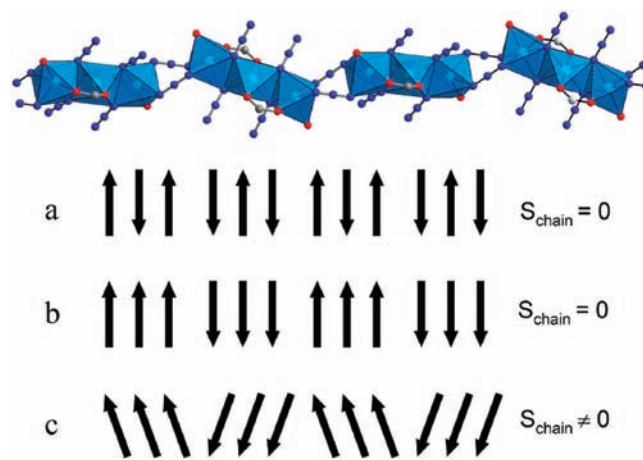


Figure 9. Field-dependent isothermal magnetization curve for compound **5** at 2 K (the solid line is a guide for the eye).

Chart 2



sufficient to overcome the spin canting, and the correlation between the canted spins leads to the ferromagnetic-like behaviors revealed by the temperature and field-dependent measurements. Notably, spin canting may also occur within the FM trinuclear unit because there is also no inversion center between the neighboring metal ions linked by the triple bridge, and the metal chromophores are also tilted toward each other. But this type of spin canting is neither necessary nor sufficient to explain the observed behaviors of **5**. Further magnetic measurements (Figures S7 and S8, Supporting Information) including field- and zero-field-cooled magnetization, hysteresis, and ac susceptibility suggested that **5** does not exhibit long-range ordering above 2 K. Magnetic measurements at still lower temperatures are needed to observe the possible long-range ordering behaviors, which often accompany spin canting.

Although isomorphous with **5**, **4** shows no indications of spin canting above 2 K. This may be because the magnetic anisotropy of Mn(II) in **4** is too small to cause canting above 2 K. It is noted that there have been some literature examples of isomorphous systems in which the Co(II) species exhibit spin canting but the Mn(II) species do not.^{20,36}

Conclusions

We have described the structures and magnetic properties of five Mn(II), Co(II), and Ni(II) compounds with mixed

(34) (a) Li, R. Y.; Wang, X.-Y.; Liu, T.; Xu, H.-B.; Zhao, F.; Wang, Z.-M.; Gao, S. *Inorg. Chem.* **2008**, *47*, 8134. (b) Viau, G.; Lombardi, M. G.; Munno, G. D.; Julve, M.; Lloret, F.; Faus, J.; Caneschi, A.; Clemente-Juan, J. M. *Chem. Commun.* **1997**, 1195.

(35) (a) Dzyaloshinsky, I. *J. Phys. Chem. Solids* **1958**, *4*, 241. (b) Moriya, T. *Phys. Rev.* **1960**, *120*, 91. (c) Moriya, T. *Phys. Rev.* **1960**, *117*, 635.

(36) Jia, Q.-X.; Wang, Y.-Q.; Yue, Q.; Wang, Q.-L.; Gao, E.-Q. *Chem. Commun.* **2008**, 4894.

azide and zwitterionic dicarboxylate ligands. In the isomorphous compounds **1–3**, the anionic uniform chains with mixed triple bridges (two EO azides and a syn–syn carboxylate) are cross-linked by the cationic 4,4'-trimethylenedipyridinium spacers to 2D coordination layers. These compounds represent a rare series of uniform chains with such triple bridges. With this series of isomorphous compounds with very minor structural differences, we are able to explore the nature of the magnetic interactions through the same triple bridges for different metal ions. It has been demonstrated that the Mn(II) compound displays AFM coupling through the triple bridge, while FM coupling is observed in the Co(II) and Ni(II) species. The differences have been discussed in terms of the collaboration or competition between the carboxylate and azide pathways. The isomorphous compounds **4** and **5** contain alternating chains with the unprecedented bridging network in which triple (two EO azides plus a carboxylate)

and double (two EE azides) bridges alternate in the triple–triple–double sequence. The 4,4'-dipyridinium spacers in **4** and **5** serve as side bridges along the chain, instead of linkers between chains. Magnetic analyses support alternating AFM interactions in **4**, while alternating FM–FM–AFM interactions with spin canting are suggested for **5**.

Acknowledgment. The authors thank NSFC (20571026 and 20771038), Shanghai Leading Academic Discipline Project (B409), and STCSM (06SR07101) for financial support.

Supporting Information Available: Crystallographic data in CIF format; selected bond parameters, powder X-ray diffraction, supplementary structural graphics, and magnetic plots in PDF format are available. This material is available free of charge via the Internet at <http://pubs.acs.org>.